14th Australasian Fluid Mechanics Conference
Adelaide University, Adelaide, Australia
10-14 December 2001

Potential Vorticity "Crises" and Western Boundary Current Separation

A. E. Kiss

Research School of Earth Sciences
Australian National University, Canberra, ACT 0200, AUSTRALIA

Abstract

Process studies have shown that western boundary currents of wind-driven midlatitude oceanic gyres can separate from the coast in response to a change in sign of the wind stress curl, a collision with another western boundary current, outcropping of isopycnals or an abrupt change in bottom topography or boundary shape. However western boundary current separation is also observed in the "sliced cylinder" model of a wind-driven gyre in a circular basin, even though this very simple model lacks all of these features.

We present numerical results which reveal the distribution of potential vorticity production and dissipation in this model and shed light on the dynamics responsible for the "unprovoked" separation. It has been suggested that a "crisis" due to insufficient recovery of potential vorticity Q in the outer boundary current outflow can result in separation. However our numerical results demonstrate that in fact the "crisis" occurs in the viscous sublayer of the western boundary current, where fluid columns acquire more Q than they lost in the interior. The outflow must therefore dissipate this excess Q before merging with the interior flow. Under strongly nonlinear conditions sufficient viscous dissipation of Q can only be obtained when the outflow separates from the boundary.

Introduction

At mid-latitudes the large-scale mean horizontal circulation of the upper ocean is dominated by gyres driven by the surface wind stress curl. These recirculations span the width of ocean basins, with slow meridional flow in most of the basin returned by narrow, rapid boundary currents at the western side. These currents separate from the coast at some point and meander across the interior between the gyres.

The question of what processes control the separation of western boundary currents (WBCs) has attracted significant attention over the years, particularly because inaccurate prediction of the separation site has been a persistent problem in ocean general circulation models [9]. Among the factors which have been shown to influence separation in particular models are a change in sign of the wind stress curl [11], a collision with another WBC [4], outcropping of isopycnals [13] or a sudden change in bottom topography or boundary shape [5, 14].

In order to address this issue, we investigate the dynamics of the flow in the sliced cylinder, the simplest mid-latitude gyre model in which separation has been observed [1, 2, 6]. This "lowest common denominator" model lacks most of the features associated with separation in other models. The mechanism responsible for the apparently "unprovoked" separation is therefore of interest, as it could also operate in more dynamically complex models.

The "sliced cylinder" model

The sliced cylinder [1, 16] is a laboratory model which captures some of the essential dynamics of mid-latitude wind-driven circulation. The apparatus (shown in figure 1) is a tank filled with water which rotates with a constant angular velocity $\Omega\hat{\mathbf{k}}$ about a vertical axis. The rigid horizontal lid has a slightly different angular velocity $(1+\epsilon)\,\Omega\hat{\mathbf{k}}$ in order to simulate a spatially uniform wind stress curl. The sloping planar bottom produces a potential vorticity gradient which is analogous to that of a β-plane and allows us to identify directions in the apparatus with various points of the compass, as shown in figure 1 (note that the apparatus rotates in the northern hemisphere sense). The numerical experiments reported here are simulations of the laboratory experiments of Griffiths [6], whose apparatus had a width $2a = 98.0$ cm, a mean depth $H_o = 12.5$ cm, and a bottom slope $s = 0.1$.

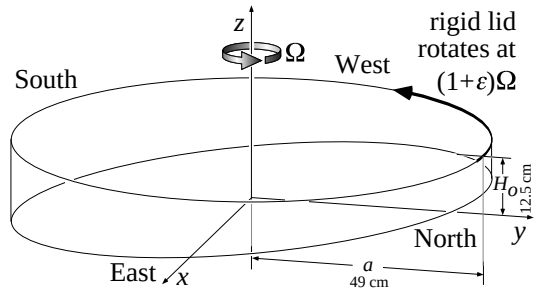

Figure 1: Perspective diagram of the "sliced cylinder" model used in the laboratory and numerical experiments.

Formulation

A detailed derivation of the formulation used in this numerical study is given in [8]; only a sketch is included here. The flow of an incompressible homogeneous fluid in a frame of reference rotating with constant angular velocity $\Omega\hat{\mathbf{k}}$ is governed by the momentum equation

$$Ro\left[\frac{\partial \mathbf{u}}{\partial t} + (\mathbf{u}\cdot\nabla)\,\mathbf{u}\right] + 2\hat{\mathbf{k}}\times\mathbf{u} = -\nabla p + E\nabla^2\mathbf{u} \qquad (1)$$

and the continuity equation $\nabla\cdot\mathbf{u} = 0$, where $\mathbf{u}$ is the velocity, p is the pressure and $\hat{\mathbf{k}}$ is the unit vector in the z direction (vertical). The length, time, velocity and pressure have been scaled by H_o, $|\epsilon\Omega|^{-1}$, $|\epsilon\Omega|H_o$ and $|\epsilon|\Omega^2 H_o^2\rho$, respectively, where ρ is the density of the fluid (all quantities introduced in this paper have been scaled in this way unless otherwise noted). The importance of advection and viscosity are parameterised by the Rossby number $Ro = |\epsilon|$ and Ekman number $E = \frac{\nu}{\Omega H_o^2}$, respectively, where ν is the kinematic viscosity of the fluid. With this scaling the radius of the tank is $\Lambda = \frac{a}{H_o}$ and the top and bottom boundaries are at $z = 1$ and $z = sy$.

We are interested in the parameter ranges $0 < Ro < 0.2$, $10^{-5} < E < 10^{-3}$ and $\Lambda \approx 4$ corresponding to those

used in the laboratory experiments of Griffiths [6]. We aim to derive equations governing the horizontal flow in the bulk of the fluid, outside the thin ($O(E^{\frac{1}{2}})$) Ekman layers on the top and bottom boundaries and the Stewartson $E^{\frac{1}{3}}$ sidewall layer. With these parameter ranges the horizontal flow in this region is depth-independent, and very nearly horizontally nondivergent. As a consequence of depth-independence, the vertical component of the curl of equation (1) yields the vorticity equation

$$Ro\left[\frac{\partial\zeta}{\partial t}+\nabla_H\cdot(\mathbf{u}_H\zeta)\right]-2\frac{\partial w}{\partial z}=E\nabla_H^2\zeta, \qquad (2)$$

where $\zeta=\hat{\mathbf{k}}\cdot\nabla\times\mathbf{u}$ is the vorticity, w is the vertical velocity, $\mathbf{u}_H$ is the horizontal velocity, and ∇_H is the horizontal gradient operator.

The continuity equation implies that $\frac{\partial w}{\partial z}$ is independent of depth in a region where $\frac{\partial \mathbf{u}_H}{\partial z}=\mathbf{0}$, and can therefore be determined from the steady, linear Ekman matching conditions for w at the top and bottom of this region. We also neglect the small divergent component of the horizontal velocity in the advection and orographic terms, to obtain the vorticity equation

$$\mathtt{T}+\mathtt{A}+\mathtt{O}+\mathtt{W}+\mathtt{E}+\mathtt{V}=0, \qquad (3)$$

where $\mathtt{T}=-Ro\frac{\partial\zeta}{\partial t}$ is the time-dependence, $\mathtt{A}=-Ro\nabla_H\cdot(\mathbf{u}_\psi\zeta)$ is the advection, $\mathtt{O}=2\nabla_H\cdot(\mathbf{u}_\psi\ln D)$ is the orographic stretching, $\mathtt{W}=2E^{\frac{1}{2}}\epsilon/(|\epsilon|D)$ is the "wind" forcing (Ekman pumping by the lid), $\mathtt{E}=-2E^{\frac{1}{2}}\zeta/D$ is the Ekman friction, and $\mathtt{V}=E\nabla_H^2\zeta$ is the lateral viscous dissipation ($\mathbf{u}_\psi=\hat{\mathbf{k}}\times\nabla_H\psi$ is the nondivergent part of $\mathbf{u}_H$ and $D=1-sy$ is the scaled fluid depth). Together with the Poisson equation $\zeta=\nabla_H^2\psi$ and the no-slip boundary condition $\psi=\frac{\partial\psi}{\partial r}=0$ at $r=\Lambda$ we have a closed system for the evaluation of the streamfunction ψ.

The numerical model

The numerical model was based on a code developed by Page [12], which was modified to solve (3) using conservative finite differences on a polar grid. The alternating-direction implicit method was used for temporal advancement, and the Poisson equation was solved for ψ using a direct method based on a fast Fourier transform in θ. An in-timestep iteration served to converge ζ at the boundary to a value which was consistent with the no-slip boundary condition, and also to allow relaxation of the advective term which couples ψ and ζ. The code is described in detail in [8]. The numerical results reported here were obtained using a uniform grid with 160 radial and 512 azimuthal points, and a timestep of $10^{-3}E^{-\frac{1}{2}}$ rotation periods. The integration was continued until the flow had adjusted to its asymptotic state (a steady circulation for the results reported here). The accuracy of the calculated results was confirmed by detailed comparisons with laboratory experiments [6, 8].

Results and Analysis

Under anticyclonic forcing ($\mathtt{W}<0$), there is a broad, slow southward flow in the interior (in a topographic Sverdrup balance between $\mathtt{W}$ and $\mathtt{O}$) which is returned by a narrow, rapid northward current against the western boundary. The Sverdrup flow is almost irrotational, and the western boundary current is mostly anticyclonic, except for a thin, strongly cyclonic viscous sublayer against the boundary (see figure 2 (a–c)). When $Ro=0$ the circulation has north-south symmetry. As Ro is increased, the WBC becomes intensified in the north, then separates from the boundary as a jet at large Ro. At first the separation takes place without any recirculation at the boundary (see figure 2 (b); note that ζ does not change sign at the boundary), but at larger Ro a recirculation "bubble" appears as in figure 2 (c).

Separation Criteria

Two different criteria can be used to characterise the onset of separation [2]: **1** a change in sign of ζ at the boundary (this is the conventional criterion, indicating a stagnation point at the boundary and a region of reversed flow along the boundary), or **2** a change in sign of $\partial\zeta/\partial r$ at the boundary (indicating a region of high vorticity extending into the interior and a breakdown of the boundary-layer approximation where $\partial\zeta/\partial r=0$). **2** is the weaker criterion, as it occurs at lower Ro than that required to produce reversed flow [6, 8]. When both criteria are satisfied, the point at the boundary where $\partial\zeta/\partial r=0$ is always upstream of the point where $\zeta=0$. The flow in figure 2 (a) does not satisfy either criterion; figure 2 (b) shows separation by criterion **2** but not **1** (separation without recirculation), and figure 2 (c) shows separation by both criteria.

Potential Vorticity

The first three terms of equation (3) conserve the potential vorticity $Q=Ro\zeta-2\ln D$. Contours of Q therefore act to steer the flow, since fluid columns can only cross Q contours when subjected to a net torque from the Ekman and viscous terms $\mathtt{W}$, $\mathtt{E}$ and $\mathtt{V}$. When $Ro=0$ the potential vorticity structure is determined purely by the bathymetry, so Q is high in the north and low in the south and has no zonal variation. At nonzero Ro, Q is modified by ζ; the plots of ζ indicate the difference in Q/Ro between the WBC and the irrotational Sverdrup interior at the same "latitude". The strongly cyclonic vorticity in the viscous sublayer increases Q against the western boundary, so Q contours are deflected southwards. In contrast, there is a northward deflection of Q contours in the anticyclonic outer WBC.

The anticyclonic surface "wind" stress reduces the Q of fluid columns by driving them southwards in the Sverdrup interior; this change must be balanced by an equal and opposite increase of Q on each streamline in the return flow in the WBC. The locations where these Q changes occur can be determined from plots of the change in Q per unit arc length S along a streamline, which is equivalent to the gradient of Q in the direction of $\mathbf{u}_\psi$:

$$\begin{aligned}\frac{\partial Q}{\partial S}&=\left(\frac{\mathbf{u}_\psi}{|\mathbf{u}_\psi|}\right)\cdot\nabla_H Q\\&=(\mathtt{W}+\mathtt{E}+\mathtt{V})/|\mathbf{u}_\psi|\\&=-(\mathtt{A}+\mathtt{O})/|\mathbf{u}_\psi|,\end{aligned} \qquad (4)$$

where the second and third lines follow from equation (3) in the steady state. $\frac{\partial Q}{\partial S}$ is plotted in figure 2 (d–f).

At nonzero Ro the distortion of Q contours means that fluid in the cyclonic sublayer must regain its Q earlier than when $Ro=0$ if it is to remain close to the boundary. In contrast, the Q recovery is delayed for the flow in the outer WBC. This results in a relative shift in the regions of positive $\frac{\partial Q}{\partial S}$ in the inner and outer parts of the

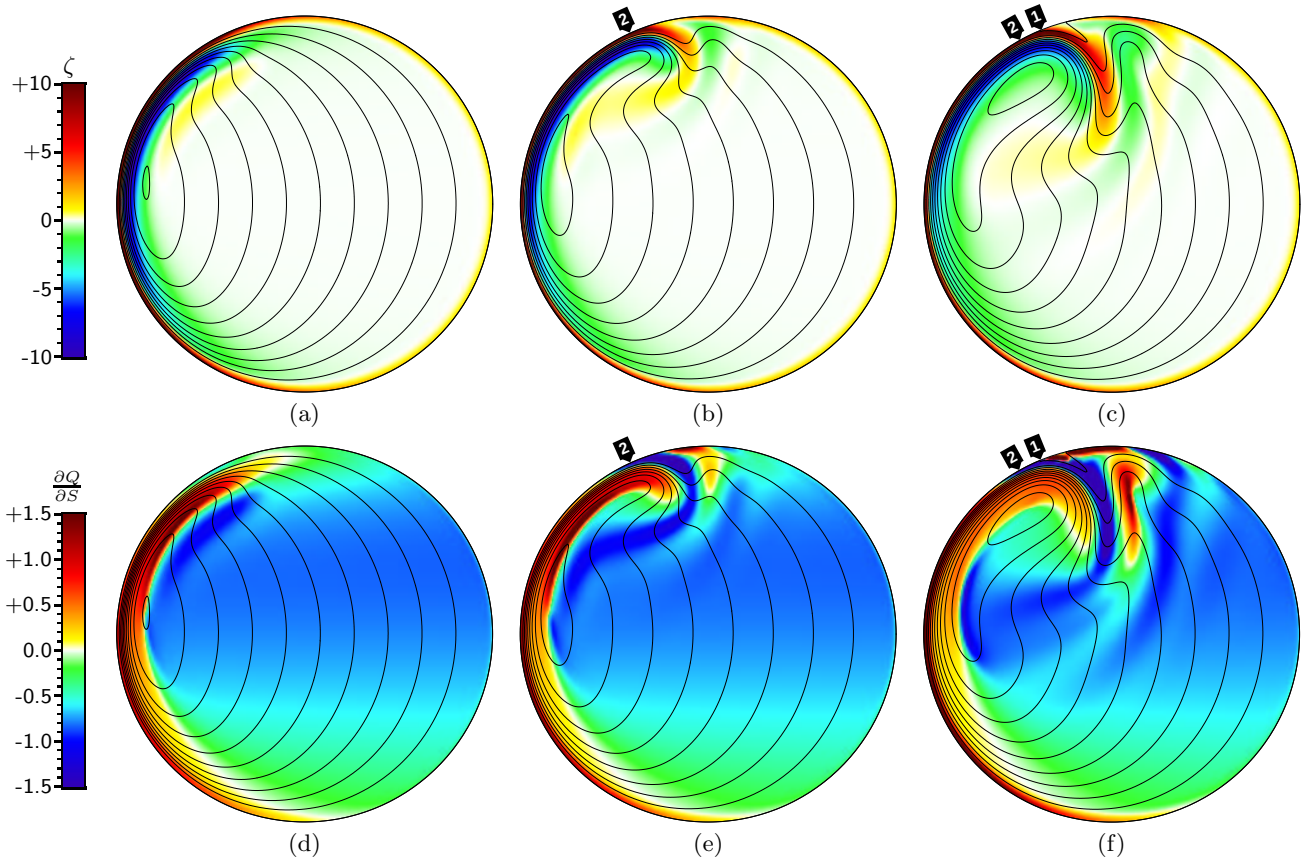

Figure 2: Relative vorticity (top) and production and dissipation of potential vorticity (bottom) in the sliced cylinder with $s = 0.1$ and $\Lambda = 3.92$. (a,d): $Ro = 2.0 \times 10^{-2}$, $E = 12.5 \times 10^{-5}$; (b,e): $Ro = 4.0 \times 10^{-2}$, $E = 8.87 \times 10^{-5}$; (c,f): $Ro = 8.32 \times 10^{-2}$, $E = 12.5 \times 10^{-5}$. The contour interval in ψ is $5 \times 10^{-3}\Lambda^2$. North is at the top, and the circulations are clockwise and steady. The westernmost points satisfying criteria **1** and **2** are marked.

boundary current, as is evident in figure 2 (d): this region is shifted upstream (southwards) in the inner boundary current, and downstream in the outer boundary current.

Although all the fluid columns must have a net recovery of the Q they lost in traversing the interior, even at moderate Ro the strength of the cyclonic vorticity in the sublayer leads to a potential vorticity that exceeds that in the northern Sverdrup region. Thus fluid that returns via the sublayer will acquire excess Q that must be dissipated in the sublayer outflow. This results in the region of negative $\frac{\partial Q}{\partial S}$ in the cyclonic part of the outflow in figure 2. The Q surplus in the sublayer becomes greater as Ro is increased, and the increased Q dissipation requires an appropriate vorticity distribution in the WBC outflow region. It will be shown here that at large Ro the dissipation of the excess Q becomes a "crisis" which is resolved by separation of the WBC.

We will assume for now that there is no recirculation, so the flow along the boundary is northward and the no-slip condition implies $\zeta > 0$ at the boundary. In the inflow region of the sublayer $\mathtt{V}$ is positive whilst $\mathtt{E}$ and $\mathtt{W}$ are negative, and $\mathtt{W}+\mathtt{E}+\mathtt{V} > 0$. It is evident from equation (4) that a reduction in Q requires $\mathtt{W}+\mathtt{E}+\mathtt{V} < 0$, but at first glance it is difficult to say whether this will take place by $\mathtt{V}$ becoming less positive, or $\mathtt{E}$ becoming more negative. However equation (4) also shows that $\mathtt{A}+\mathtt{O} > 0$ in a region of Q reduction; since the flow is northwards we have $\mathtt{O} < 0$, so $-\mathtt{A} < \mathtt{O} < 0$. Now $\mathtt{A} = -Ro|\mathbf{u}_\psi|\frac{\partial \zeta}{\partial S}$ and $\mathtt{O} = 2|\mathbf{u}_\psi|\frac{\partial \ln D}{\partial S}$, so $\frac{\partial \zeta}{\partial S} < \frac{2}{Ro}\frac{\partial \ln D}{\partial S} < 0$. Thus ζ decreases downstream at a finite rate; by continuity we must also have $\frac{\partial \zeta}{\partial S} < 0$ for some distance upstream of the region where $\frac{\partial Q}{\partial S} < 0$. Since $\frac{\partial \zeta}{\partial S} < 0$ and $\zeta > 0$, $\mathtt{E}$ becomes *less* negative as the flow enters the dissipation region ([8] showed that this occurs despite the decrease in D if $Ro < \frac{2}{\zeta}$, which is the case here). Thus $\mathtt{V}$ must decrease in order to obtain $\mathtt{W}+\mathtt{E}+\mathtt{V} < 0$ in the sublayer outflow.

If we make the boundary-layer approximation we have $E\nabla_H^2\zeta \approx E\left(r^{-1}\partial\zeta/\partial r + \partial^2\zeta/\partial r^2\right)$. Upstream of the region where $\frac{\partial Q}{\partial S} < 0$, ζ decreases monotonically away from the boundary, at a decreasing rate, so $\mathtt{V} > 0$. As the fluid columns pass into the Q dissipation region, $\frac{\partial Q}{\partial S}$ becomes negative via a small change to the vorticity profile which reduces $\mathtt{V}$ below $-(\mathtt{W}+\mathtt{E})$ but does not change its sign. At small Rossby number this low rate of Q loss is sufficient to adjust the potential vorticity of fluid columns to a value which allows them to re-enter the interior, and no more drastic alterations are needed (see figure 2 (d)). As Ro increases, $\frac{\partial Q}{\partial S}$ must become more negative in the sublayer outflow, since the Q surplus is larger. Eventually at large Ro, $\frac{\partial Q}{\partial S}$ needs to decrease to a value which can only be obtained if $\mathtt{V} < 0$. While it is possible at first to have $\mathtt{V} < 0$ while retaining the cross-stream maximum in ζ at the boundary, further downstream the vorticity maximum tends to leave the boundary, so that $\partial^2\zeta/\partial r^2$ and $\partial\zeta/\partial r$ are both negative between the boundary and the vorticity maximum ($\frac{\partial^2\zeta}{\partial\theta^2}$ makes an insignificant contribution to $\mathtt{V}$). This separation of the ζ maximum can be seen in figure 2 (b,c) past the point marked **2**.

The displacement of the ζ maximum offshore changes the

sign of $\partial\zeta/\partial r$ at the boundary, which is flow separation by criterion **2**. Separation of the vorticity maximum creates a bulge in the Q contours, so the region of large Q also extends away from the boundary. By definition, streamlines in the region where $\frac{\partial Q}{\partial S} < 0$ must cross potential vorticity contours in the direction of decreasing Q; as a result, the streamlines on the "seaward" side of the bulge are guided away from the boundary, and the anticyclonic outer part of the WBC is also deflected offshore as a result. When the resulting offshore flow is sufficiently inertial it advects the layers of positive and negative ζ into the interior to form a jet (see figure 2 (b)). In contrast the fluid very close to the sidewall ends up on the "shoreward" side of the bulge in the Q contours past the point where $\partial\zeta/\partial r = 0$. This fluid does not separate (at least at first) but creeps northward near the boundary in the nearly stagnant region north of the separated jet. Very little fluid takes this second route under the conditions shown.

Figure 2 shows that the unseparated part of the sublayer is flowing into a region of decreasing Q, so ζ continues to decrease with distance along the boundary past the point marked **2**. When Ro is sufficiently large ζ decreases so rapidly past this point that a region of anticyclonic vorticity is formed at the boundary (see figure 2 (c)), giving separation by criterion **1** where $\zeta = 0$. This picture of the separation process explains the observation that recirculation only occurs when there is a point upstream where $\partial\zeta/\partial r = 0$. It also explains why separation does not occur under the free-slip boundary condition [3, 8], since in that case the cyclonic sublayer is absent, and a "crisis" of Q dissipation does not occur.

Summary and Conclusions

WBC separation in the sliced cylinder can be explained as an adjustment process which allows the outflow which passes close to the sidewall to change its potential vorticity to match that in the interior. This adjustment requires a region of Q dissipation, which is facilitated at large Ro by a change in sign of $\partial\zeta/\partial r$ at the boundary. This in turn results in a Q structure which guides the flow away from the boundary, but need not result in the formation of a recirculation region. A change in sign of $\partial\zeta/\partial r$ at the boundary is fundamental to the WBC separation process, and a necessary precursor to separation with recirculation. From this point of view the formation of a recirculation region is of little fundamental importance, as it is simply a finite-amplitude expression of the vorticity dynamics required for the vorticity maximum to leave the boundary. This separation mechanism differs from that suggested previously [7, 15] in that the potential vorticity "crisis" occurs in the sublayer due to an excessive recovery of Q, rather than in the outer boundary current due to insufficient Q recovery.

We note that the separation process described here requires only lateral viscosity, vorticity advection and an ambient potential vorticity gradient, so the arguments presented above apply equally well if `E` and/or `W` are omitted. Analogous potential vorticity considerations also apply under cyclonic forcing ($\mathtt{W} > 0$), causing separation of the WBC outflow in the southwest at large Ro. The general mechanism does not depend on the particular formulation used here, or the functional form of the potential vorticity. This process may therefore be relevant to separation of western boundary currents in other models. For example, Moro [10] noted that a change in sign of the lateral viscous diffusion was associated with separation in a two-gyre model with no-slip boundary conditions and no bottom friction. In his results the bulk of the streamlines leave the boundary well upstream of the stagnation point, in a region where both the lateral viscous diffusion and the normal gradient of the vorticity change sign. These general features are analogous to those identified in the sliced cylinder. It is possible that a similar process plays a role in WBC separation in the oceans, although the dynamics are likely to be much more complex due to isopycnal outcropping, spatially variable forcing and complex topography.

References

[1] Beardsley, R. C., A laboratory model of the wind-driven ocean circulation, *J. Fluid Mech.*, **38**, 1969, 255–271.

[2] Becker, A. and Page, M. A., Flow separation and unsteadiness in a rotating sliced cylinder, *Geophys. Astrophys. Fluid Dyn.*, **55**, 1990, 89–115.

[3] Blandford, R. R., Boundary conditions in homogeneous ocean models, *Deep-Sea Res.*, **18**, 1971, 739–751.

[4] Cessi, P., Laminar separation of colliding western boundary currents, *J. Mar. Res.*, **49**, 1991, 697–717.

[5] Dengg, J., The problem of Gulf Stream separation: A barotropic approach, *J. Phys. Oceanogr.*, **23**, 1993, 2182–2200.

[6] Griffiths, R. W. and Kiss, A. E., Flow regimes in a wide 'sliced-cylinder' model of homogeneous β-plane circulation, *J. Fluid Mech.*, **399**, 1999, 205–236.

[7] Holland, W. R. and Lin, L. B., On the generation of mesoscale eddies and their contribution to the oceanic general circulation. II: A parameter study, *J. Phys. Oceanogr.*, **5**, 1975, 658–669.

[8] Kiss, A. E., *Dynamics of laboratory models of the wind-driven ocean circulation*, PhD thesis, Australian National University, 2000.

[9] McWilliams, J. C., Modeling the oceanic general circulation, *Ann. Rev. Fluid Mech.*, **28**, 1996, 215–248.

[10] Moro, B., On the nonlinear Munk model, I: Steady flows, *Dyn. Atmos. Oceans*, **12**, 1988, 259–287.

[11] Munk, W. H., On the wind-driven ocean circulation, *J. Meteorology*, **7**, 1950, 79–93.

[12] Page, M. A., A numerical study of detached shear layers in a rotating sliced cylinder, *Geophys. Astrophys. Fluid Dyn.*, **22**, 1982, 51–69.

[13] Parsons, A. T., A two-layer model of Gulf Stream separation, *J. Fluid Mech.*, **39**, 1969, 511–528.

[14] Pedlosky, J., A necessary condition for the existence of an inertial boundary layer in a baroclinic ocean, *J. Mar. Res.*, **23**, 1965, 69–72.

[15] Pedlosky, J., On Parsons' model of the ocean circulation, *J. Phys. Oceanogr.*, **17**, 1987, 1571–1582.

[16] Pedlosky, J. and Greenspan, H. P., A simple laboratory model for the oceanic circulation, *J. Fluid Mech.*, **27**, 1967, 291–304.